A novel charged-particle diagnostic for compression in inertial confinement fusion targets

P. B. Radha and S. Skupsky
Laboratory for Laser Energetics, University of Rochester, 250 East River Road, Rochester, New York 14623-1299

R. D. Petrasso
Plasma Science and Fusion Center, MIT, Cambridge, Massachusetts 02139

J. M. Soures
Laboratory for Laser Energetics, University of Rochester, 250 East River Road, Rochester, New York 14623-1299

A new technique for diagnosing compression in multiple regions of inertial confinement fusion targets is discussed. This diagnostic uses knock-on deuterons and protons that have been elastically scattered by 14.1 MeV deuterium–tritium (DT) fusion neutrons. The target is composed of three different materials: DT gas contained in a plastic shell overcoated by deuterated plastic. The effect on the knock-on deuteron spectrum of mixing of these layers from hydrodynamic instabilities is also discussed. © *2000 American Institute of Physics.* [S1070-664X(00)01904-2]

I. INTRODUCTION

Areal density—the product of density and thickness (ρR) of specific materials or regions in inertial confinement fusion (ICF) targets—is an important measure of compression that enables a comparison between ICF implosions and simulation. In particular, this quantity influences several crucial aspects of an igniting target: the degree of self-heating in the target, its fractional burn, and gain.[1]

Several methods involving nuclear reaction products have been employed to determine ρR in ICF implosions.[2–5] In this article, we will discuss the use of knock-on particles (deuterons and protons) that have been elastically scattered from the 14 MeV primary deuterium–tritium (DT) fusion neutrons. Both knock-on deuterons[2,3] and protons[5] have been previously used as a means of inferring the areal density of a single region of the target, namely, the fuel. The primary focus of this paper is a novel knock-on deuteron-based diagnostic that will simultaneously diagnose *multiple* regions of a compressed target. The knock-on proton spectrum will also be used to independently infer areal density for one of the regions, and thereby provide a self-consistency check.

The target consists of DT gas enclosed in a plastic (CH) shell overcoated by a layer of deuterated plastic (CD) and is of interest because its characteristics are commensurate with the targets surrogate[6] to future cryogenic targets planned for the OMEGA laser.[7] The central goal of the cryogenic targets is to validate the performance of the high-gain direct-drive ignition designs planned for use on the National Ignition Facility. Experiments with surrogate targets can offer a larger array of diagnostic techniques to provide useful information on target behavior.

In a direct-drive ICF target implosion, degradation in target performance is believed to occur primarily through the Rayleigh–Taylor instability,[8] which is seeded by either target imperfections or laser nonuniformity. This instability, oc-curring at the ablation surface, can then feed through to the fuel–shell interface during the acceleration phase of the implosion and add to any preexisting roughness on the inner surface. During the deceleration phase, these distortions at the fuel–shell interface can grow, resulting in a mixing of the fuel and the shell material. The knock-on particle spectrum carries information about conditions in the target during this latter phase of the implosion. This is when core temperatures and densities are high enough to initiate the fusion process and to produce the knock-on ions. The mixing of the fuel and the shell at these times in the implosion can significantly modify the neutron production rate relative to ideal one-dimensional (1-D) simulations, and consequently the production of the knock-on ions and their spectra. This diagnostic as a result will probe conditions in the target at different times relative to 1-D simulations, depending on the extent of mixing. Other diagnostic tools such as the neutron temporal diagnostic (NTD)[9] (which can measure the thermonuclear burn history of a target in an experiment) can provide information on the time of neutron production, and consequently the time during the implosion that the ρR is determined.

Current diagnostics on the mixing of various layers in the target use x-ray spectroscopic signatures from various dopants in the target.[6] Techniques based on nuclear particles would provide an independent assessment of hydrodynamic mix in the target and could probe conditions in the target that are not easily accessible by x-ray spectroscopy.

The knock-on deuteron diagnostic can provide information about the compressed target in a relatively model-independent way for values of target ρR up to ~ 100 mg/cm^2 (Ref. 2). The number of knock-on deuterons can provide information on the areal densities of the layer in which they are produced, and the energy loss of these particles as they propagate out of the target will provide additional information about ρR along the propagation path. For values of ρR

1531

higher than 100 mg/cm^2, the knock-on spectrum is significantly distorted and any inference of areal densities is very model dependent.

The knock-on proton diagnostic is somewhat similar to the knock-on deuteron diagnostic. The number of these particles is once again proportional to the areal density of the layer in which they are produced (such as the plastic shell). However, the spectrum of these particles is significantly different from the deuterons, and a different analysis must be used to interpret the measurement. In earlier work, a model-dependent technique to interpret the proton signal was presented.[5] In this paper, we present a more model-independent analysis of the proton spectrum that relies on the number of knock-on protons in a suitably defined energy range.

Maximum information from the knock-on diagnostics is obtained by using detailed information about the shape and magnitude of the knock-on spectrum. Until recently, the technique used to detect the knock-on deuterons has involved counting tracks that satisfy selective criteria in stacked track detectors, consequently providing only gross information about the particle spectrum. This lack of detailed spectral information has limited the use of knock-on ions as a diagnostic. With the deployment of the new charged-particle spectrometer (CPS),[10] detailed spectral information of charged reaction products from the imploding target can now be obtained, enabling a more complete analysis of conditions in the target using the knock-on particles. Using a 7.5-kG magnet, the CPS can momentum-select incident charged particles, which are then impinged onto a detector plane consisting of track detectors. The identity of each particle is then established by comparing the track diameters with known stopping powers of various particles at that momentum. The detailed spectra obtained in this manner have permitted measurements of areal densities in ICF targets.[11]

In the sections that follow, we first discuss (Sec. II) the knock-on particles from a typical target that consists of only two regions: DT fuel and a plastic (CH) shell. Knock-on deuterons (and tritons) are produced in the fuel, and knock-on protons are produced in the CH shell. The analysis of each of these is discussed. A generalization of this technique to infer ρR in three regions of the compressed target, using the detailed shape of the deuteron spectrum, is described in Sec. III. The target is fabricated from three materials: DT fuel is enclosed in a CH shell overcoated with CD. Knock-on deuterons are produced in both the DT and CD layers with two well-defined high-energy peaks in the spectrum, separated by an energy determined by the areal density of the intermediate CH layer. Using the results from simulation as examples, we demonstrate the procedure for deducing the ρR of the three layers from the deuteron spectrum. In Sec. IV, we discuss how hydrodynamic instabilities could modify the measured knock-on deuteron spectrum and examine the validity of our analysis for the modified spectra.

II. KNOCK-ON IONS AS A DIAGNOSTIC FOR ρR

The knock-on diagnostic relies on the elastic scattering of various ions (deuterons and protons) in the target from the
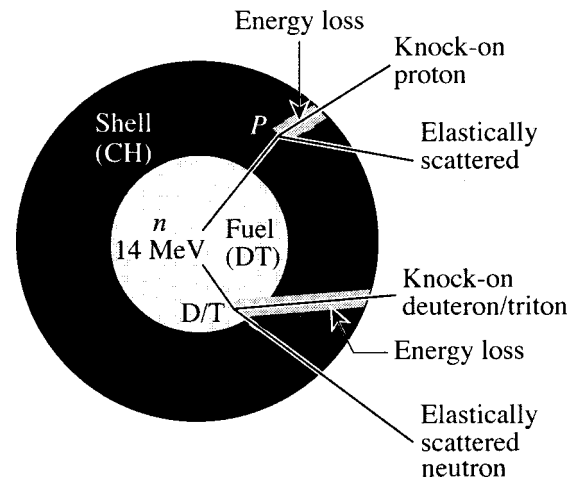

FIG. 1. Knock-on process: The elastic scattering with the primary DT neutrons produces ''knock-on'' particles (deuterons, tritons, and protons), which lose energy as they transverse the target.

14.1 MeV primary DT neutrons (Fig. 1). The number of such elastically scattered particles, N_K, is then proportional to the number of primary neutrons, Y, the number density for the particle of interest, n_K, the average distance that the neutron traverses in the target, $\langle R \rangle$, and is given by

$$N_K = n_K \langle R \rangle \sigma_K Y, \qquad (1)$$

where the subscript K indicates the type of knock-on particle, and σ_K is the corresponding cross section for elastic scattering (0.64b for deuterons and 0.69b for protons). Using the relation between the ion number density and the mass density, this can be rewritten for the number of knock-on deuterons produced in equimolar DT as

$$N_D = 7.7 \times 10^{-2} Y \langle \rho R \rangle \text{ cm}^2/\text{gm}, \qquad (2)$$

where $\langle \rho R \rangle$, the areal density, is given by

$$\langle \rho R \rangle = \int_0^R \rho \, dr. \qquad (3)$$

The ratio of the number of knock-on deuterons to the number of 14.1 MeV DT primary neutrons provides a measure of the fuel's areal density. We note that knock-on tritons can also be produced in a similar elastic-scattering process with the energetic DT neutrons. However, since tritons are more massive, they move more slowly and lose energy more rapidly. Thus, their spectrum can get significantly distorted at smaller values of areal densities, leading to a less reliable inference of ρR.

Knock-on protons may be produced by the addition of hydrogen to the fuel or from the protons in the plastic (if the target is prepared with a plastic shell). For knock-on protons produced from the plastic (CH) layer, Eq. (1) for the number of elastically scattered protons can be rewritten as

$$N_p = 3.2 \times 10^{-2} Y \langle \rho R \rangle \text{ cm}^2/\text{gm}. \qquad (4)$$

Again, the ratio of the number of elastically scattered protons to the number of DT neutrons is proportional to the areal density of the plastic layer.
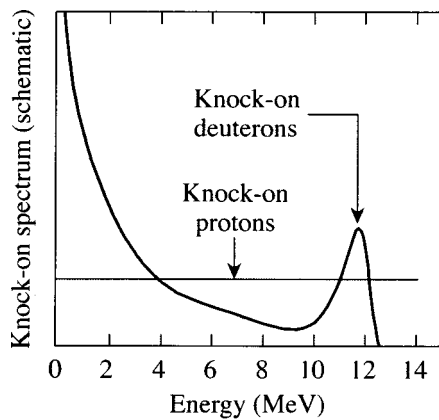
FIG. 2. Schematic spectra of the knock-on particles at production (without energy loss): The number of deuterons in the high-energy peak can be used to estimate the areal density of the layer producing the particles. Since the proton spectrum is nearly constant with energy, the number in a chosen energy range can be related to the areal density of the plastic layer.

FIG. 3. (a) The slowing down of the knock-on deuteron spectrum for different areal densities of the shell, $(\rho R)_{CH}$: The high-energy peak remains well defined for increasing slowing down of the deuterons. (b) End-point energy of the spectrum as a function of the shell's areal density: The end-point energy, defined as the higher of the half-maximum energy of the peak, is related to the shell areal density.

The challenging aspect of inferring the number of knock-ons produced relates to the spectrum of these particles. The knock-on spectrum is produced in a continuum of energies extending over several MeV (knock-on deuterons occur up to 12.5 MeV, while the proton spectrum extends up to 14.1 MeV) due to different neutron-impact parameters. The entire spectrum cannot be measured because the very low-energy knock-ons can be stopped in the target. As a result, these diagnostics rely on the identification of specific features in the high-energy portion of the knock-on spectra to deduce the total number of ions produced and hence the areal density of the layer of interest.

A. Knock-on deuterons

Even though the entire knock-on deuteron spectrum cannot be measured, the number of knock-ons produced can be reliably deduced using the high-energy region of the spectrum. The anisotropic differential cross section for elastic scattering results in a clearly identifiable peak in the spectrum (shown schematically in Fig. 2). The number of deuterons under this peak is about 16% of the total number of deuterons produced in the scattering process and is relatively independent of any distortion of the spectrum in the target over a large range of areal densities allowing for a model-independent inference of the total number of knock-on deuterons produced [and hence the ρR of the fuel, $(\rho R)_f$, through Eq. (2)].

The high-energy peak is the result of nearly "head-on" collisions between the 14 MeV neutrons and deuterons, and it determines a directional ρR along the "line-of-sight" of neutron production. Thus, two CPSs that view the target from nearly orthogonal directions should be able to detect long-wavelength variations in ρR. Such low-order modes may be imposed on the target due to power imbalance, beam mispointing, etc.,[12] and information on these modes would provide valuable feedback to laser improvements. Typical errors in the inferred ρR through CPS measurements are be-
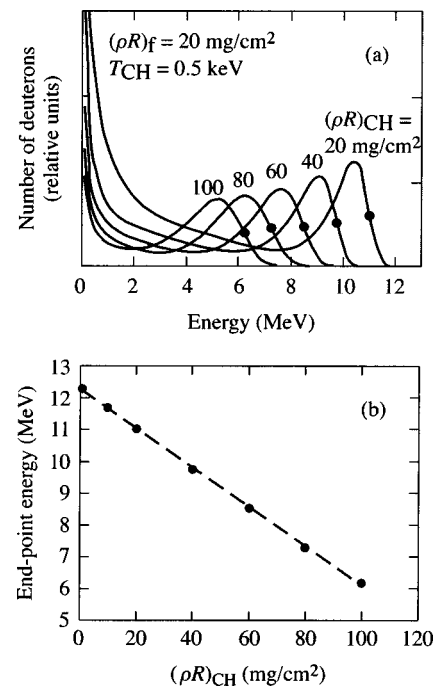
tween 10% and 20%[11] and, therefore, the knock-on technique can be practically used to deduce fuel ρR asymmetries that are larger than these errors.

In addition to the fuel areal density, the knock-on deuteron spectrum can also provide a measure of the shell's ρR. Knock-ons produced in the target slow down (primarily through energy loss in the shell), and, as a result, the spectrum is downshifted from its usual maximum of 12.5 MeV. Figure 3(a) shows the spectra due to different areal densities of the shell, $(\rho R)_{CH}$. The continuous energy loss of these charged ions is modeled using Ref. 13. The slowing down of the deuterons can be characterized by the end point of the spectrum (defined as the higher of the two energies of the half-maximum of the peak). As Fig. 3(b) indicates, this end point is proportional to the areal density of the shell.

An important feature of the knock-on deuteron diagnostic that enables a relatively model-independent measure of the shell's ρR is the temperature insensitivity of the high-energy peak of the deuteron spectrum (for $\rho R \lesssim 60$ mg/cm²). Figure 4 shows the deuteron spectra for two different shell ρR values at two different typical electron temperatures (the temperatures are typical of the shell in 1-D simulations of the implosions). Energy loss at these typical densities and temperatures in imploding ICF targets is dominated by losses to electrons (the electron density is related to the ion density and consequently the areal density of the material through its degree of ionization). Knock-on deuterons with energies greater than about 7 MeV typically have much higher velocities than electrons at the typical temperatures in the cold plastic (~0.5 keV). In this limit, the energy loss is indepen-
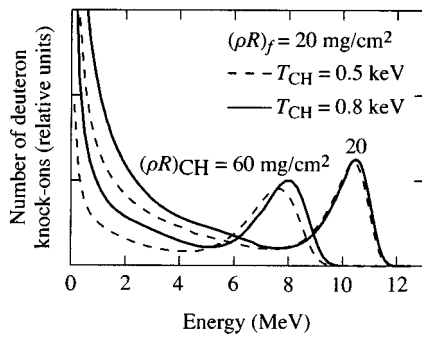
FIG. 4. The deuteron spectrum is relatively insensitive to temperatures in the cold portions of the target.

dent of the electron's temperature and is thus dependent only on the shell's ρR. As Fig. 3(a) indicates, for $\rho R \sim 60 \text{ mg/cm}^2$, the deuterons are slowed to less than 7 MeV. This value of ρR suggests a limit on the maximum value of the shell's areal density that can be deduced independent of temperature considerations in the shell. On the other hand, the knock-on tritons, being more massive, show a greater sensitivity to both the temperature and the ρR of the shell, limiting the range of temperatures and areal densities over which conditions in the target can be inferred reliably from their spectrum. The triton spectrum can be used as a self-consistency check, however, on target conditions that have been measured by other diagnostics.

B. Knock-on protons

Knock-on protons can be used independently of the deuterons to deduce the areal density of the plastic ρR_{CH}. In contrast to the knock-on deuteron spectrum, the proton knock-on spectrum is relatively flat (shown schematically in Fig. 2), making it far more difficult to relate distortion of the spectrum to ρR.

The knock-on proton spectra for various values of ρR_{CH} are shown in Fig. 5(a). The number of protons between 10.5 and 12 MeV is proportional to the areal density of the plastic and can be used to deduce ρR_{CH} up to a value of about 100 mg/cm^2 [shown in Fig. 5(b)]. The proton background from the deuteron break-up reaction $[d(n,2n)p]$ with its end point at 11.8 MeV is insignificant in the chosen energy range for target conditions of interest, primarily due to the lower cross section for the deuteron breakup reaction relative to that of the elastic scattering of protons. Thus, the number of protons measured in the chosen energy range can provide a measure of the areal density of the plastic layer.

In the next section, we consider a generalization of the knock-on deuteron diagnostic that will enable more detailed information about the compressed target.

III. "THREE-LAYER" TARGETS

The deuteron diagnostic can be extended to analyze ρR in three separate regions of the compressed target if the target has been fabricated with three different materials (Fig. 6): an inner DT (or a DT) fuel region, a plastic (CH) shell, and an ablator (CD). (Some of the CD layer is ablated by the
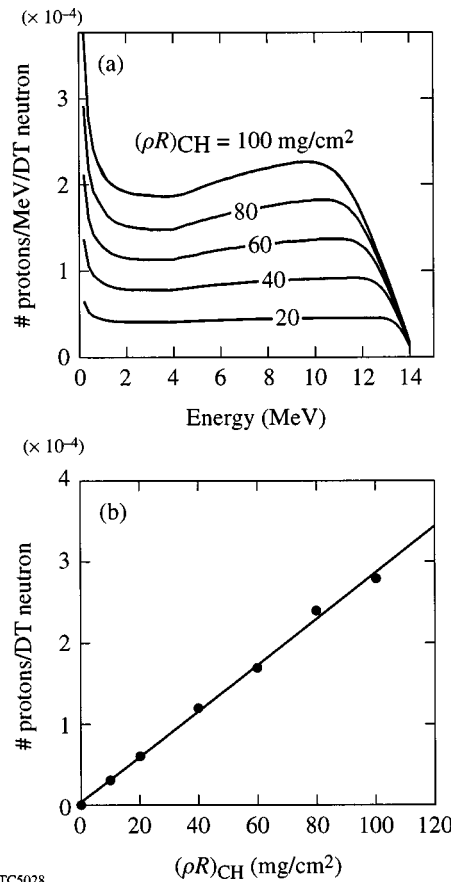
FIG. 5. (a) Proton spectra for various values of areal densities of the CH layer. (b) Number of knock-on protons between 10.5 and 12 MeV versus $(\rho R)_{CH}$: The number of protons in this energy range can be related to the areal density of the plastic layer.

laser and the remainder contributes to core compression.) The mass and size of these targets are similar to future cryogenic targets designed for the OMEGA laser. The diagnostic design permits some flexibility in each layer's thickness while retaining its equivalence to currently used cryogenic surrogate targets.

In addition to knock-on deuterons, knock-on protons are produced in the plastic (Fig. 6), and the areal density of the plastic layer can be deduced from the ratio of the number of protons produced to the number of primary neutrons.
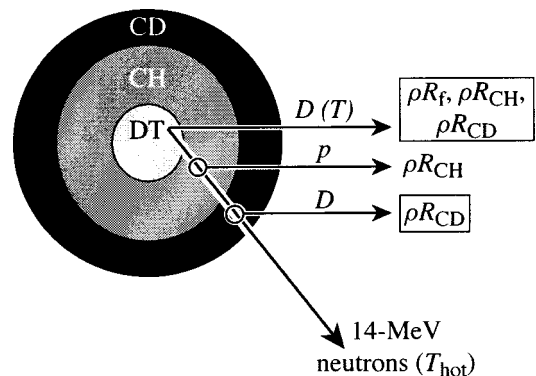

FIG. 6. Information about the areal densities of each of the layers and the temperature of the hot fuel can be inferred using the particles shown.

Phys. Plasmas, Vol. 7, No. 5, May 2000

A novel charged-particle diagnostic for compression in . . .   1535
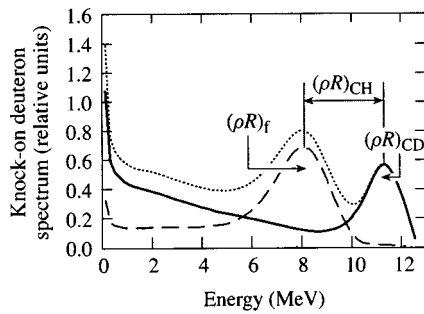

FIG. 7. Simulated knock-on deuteron spectrum from a three-layer target with contributions from the individual layers: Information about the areal densities of the three layers can be inferred from the spectrum as shown.

Knock-on deuterons are produced in both the fuel and the CD layer. The deuterons produced in the fuel lose energy as they traverse the target, causing the high-energy peak to shift downward. The spectrum of deuterons from the CD layer, on the other hand, has its maximum energy at the nascent value of 12.5 MeV. The time-integrated simulated spectrum for a target with a combined CH and CD thickness of 20 μm (5 μm CH and 15μm CD) is shown in Fig. 7. The target is driven with a 1 nsec square pulse, which is typical of many OMEGA experiments. The spectrum is produced by postprocessing a 1-D simulation of the implosion using the hydrodynamic code LILAC.[14] The postprocessor transports the knock-ons in straight lines and calculates the particle energy loss for every time step using the simulated density and temperature profiles. The relevant features are the two high-energy peaks in the spectrum arising from the individual contributions of the fuel and CD layers (shown as dashed and solid lines in Fig. 7). The area under the higher-energy peak is primarily a measure of the areal density of the CD layer, $(\rho R)_{CD}$, whereas the peak at the lower energy has contributions from both the fuel and the CD shell. The separation of the two peaks provides a measure of the areal density of the plastic layer, $(\rho R)_{CH}$.

If the peaks are well separated, the areal densities of the three layers can be deduced nearly model independently, using the scheme outlined above. We first consider the areal density of the plastic layer. For the spectrum (solid line) shown in Fig. 8(a) the separation of the two high-energy peaks is about 3 MeV. The areal density of the plastic resulting in this separation should correspond to the value that results in a downshift of the end-point energy by the same amount. From Fig. 3(b), this separation corresponds to an areal density of about 40 mg/cm^2 to be compared with the value of 35 mg/cm^2 in the simulation. Next, to deduce the areal density of the CD layer, we calculate the total number of deuterons in the high-energy peak. This value is a known fraction of the total number of deuterons produced since this portion of the spectrum is unaffected by the presence of deuterons from the fuel. For the spectrum (dashed line) in Fig. 8(a), this is the number of deuterons above 10.25 MeV, and, again, from the spectra in Fig. 3(a) this corresponds to about 12% of the total knock-on deuterons produced. Using this fraction for the number of deuterons in the peak and a formula for CD [similar to Eq. (2)], we obtain a value of 26.5
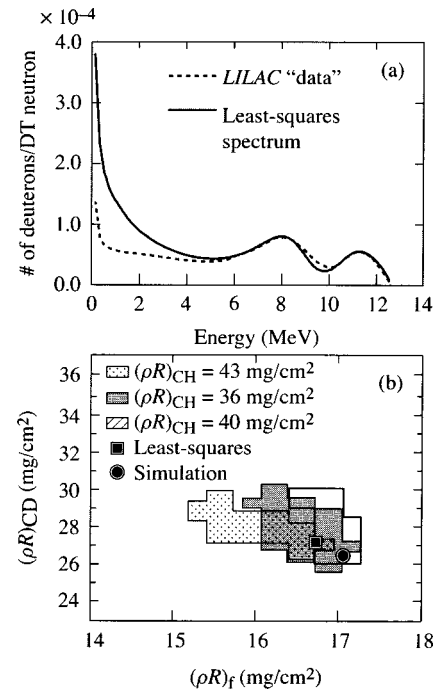

FIG. 8. (a) Comparison of test (simulated) spectrum (dashed line) showing spectrum from best-fit model (solid line). (b) Sensitivity analysis of the inferred areal densities: Shown are the areal densities for the three layers that result in spectra whose squared difference is within 20% of the least-squares values. Each shaded region represents the set of areal densities of the fuel and CD layer satisfying the 20% criterion, for a fixed value of the areal density of the CH layer.

mg/cm^2 for the CD layer that compares favorably with the value of 25.6 mg/cm^2 in the simulation. While the areal densities of the CH and CD layers can be determined model independently, some uncertainty is introduced in the value of the fuel's areal density $(\rho R)_f$ since not all the deuterons under the low-energy peak are produced in the fuel. The contribution to this peak from the CD layer depends on the slowing down of the deuterons and the geometry of the paths through the target. An upper limit for $(\rho R)_f$ can be obtained by assuming that all the deuterons under this peak are produced in the fuel. In this case, the inferred areal density of the fuel using Eq. (2) is 23.6 mg/cm^2 to be compared with the simulation value of 17.0 mg/cm^2.

A more accurate estimate of the errors in the areal densities can be obtained through the following analysis of the knock-on deuteron spectrum. We consider deuteron spectra from a model where each layer is approximated by a constant density and temperature (an ice block model). The density and the thickness of each layer are chosen by requiring a fixed mass for each layer (known from the specifications of the target being modeled) and a chosen ρR. We ignore temperatures in the colder plastic and CD in this analysis as we expect little sensitivity to these temperatures. The choice of fuel temperature, however, cannot be made arbitrarily since the deuterons may lose some energy in the hot fuel. In this example, we choose the fuel temperature at peak neutron rate in the simulation as the relevant fuel temperature. In deducing areal densities from the experimentally measured spectrum the choice of the fuel electron temperature can be

guided by the ion temperature obtained experimentally from the width of the DT neutron spectrum[15] (measured through time-of-flight techniques). It must be noted that the measured ion temperature can differ from the electron temperature, especially if the high temperature is caused by an incident shock in the fuel (which preferentially heats the ions); however, a sensitivity analysis of the spectra to this temperature can provide bounds on both the areal densities and temperatures.

In this manner we construct a static representation of the target and fit the spectra from such a model by varying the areal densities of each layer. While the ice-block model is not expected to accurately describe the primary complexities of an imploding target such as the spatial and time-dependent variation of densities and temperatures, the spatial localization of neutron sources in the target, and the geometry of the knock-on trajectories through the target, it should provide a reasonable time and spatially averaged representation of the target relevant to the knock-on spectrum.

To test our scheme for deducing the areal densities, we consider again the simulated spectrum shown as a dashed line in Fig. 8(a). Using the model described above, we vary the ρR of the three layers to minimize the least-squares difference between the spectrum from the model and the simulated data. The energy range chosen for this minimization is the area determining the two peaks in the spectrum ($\gtrsim 5$ MeV). Our chosen technique for minimization is based on the downhill simplex method of Nelder and Mead.[16] If we assume that the neutrons are created uniformly in the fuel, the resulting spectrum of such a minimization scheme is shown as the solid line in Fig. 8(a). Our values for the areal densities for the DT, CH, and CD layers (16.5, 40, and 27.4 mg/cm^2, respectively) compare favorably with the results from the simulation (17, 35, and 25.6 mg/cm^2). These values agree very well with the model-independent extraction of the areal densities of the CH and CD layers, implying correctly well-separated peaks, and, in addition, provide a tighter bound on $(\rho R)_f$.

To gauge the sensitivity of the spectrum to the least-squares values of ρR obtained in this manner, we consider Fig. 8(b), which shows sets of $(\rho R)_{CD}$ and $(\rho R)_f$ for different values of $(\rho R)_{CH}$. [Each shaded region represents a set of areal densities of CD and fuel, corresponding to a certain value of $(\rho R)_{CH}$.] For each value of $(\rho R)_{CH}$, this set corresponds to those values whose spectra are within 20% of the least-squares value. In this manner, we find the range of acceptable values of the areal densities of each layer in the target. Also shown in the figure are the least-squares value (square) and the result from the 1-D simulation (circle). We see that by using this procedure we obtain ρR values of the fuel and CD layer to within 10% of the true value. The larger range of acceptable values of $(\rho R)_{CH}$ relative to the ranges of $(\rho R)_f$ and $(\rho R)_{CD}$ indicates that the deuteron spectrum is less sensitive to the areal density of the plastic layer. This is probably due to the fact that $(\rho R)_{CH}$ does not determine an absolute number or energy, but only the relative separation of the two high-energy peaks. A comparison with the value deduced from the knock-on proton spectrum would, in addition, provide an independent check on the value of $(\rho R)_{CH}$.

Finally, we note that the true set of areal density values obtained from the simulation is not excluded from our result at this 20% level.

If we assume that the neutrons are produced in the center of the fuel (as opposed to uniformly throughout the fuel) and repeat the above analysis, we obtain the following results: an areal density of 16.3, 40.4, and 30.5 mg/cm^2 for DT, CH, and CD, respectively. The least-squares difference between the model spectra and the test data for this case is higher than for the uniform source, implying correctly a uniform distribution of the DT neutrons in the simulation.

IV. MODIFICATION OF THE KNOCK-ON DEUTERON SPECTRUM DUE TO MIX

Our discussion has been based so far on a 1-D simulation of the implosion that does not include the effects of hydrodynamic instabilities and mix on the imploding target. In addition, any effects on the target caused by long-wavelength asymmetries (possibly due to laser-beam imbalances in power and pointing errors) have also been ignored. The effects of such departures on nuclear and particle diagnostics are difficult to determine quantitatively from 1-D simulation.

During the deceleration phase, the Rayleigh–Taylor unstable fuel–shell interface, seeded by its nonuniformity, can result in a mixing of the hot fuel and cold shell. This mixing of materials at very different temperatures can result in a significant quenching of the neutron yield relative to 1-D simulations[3] (that do not include this effect). Since the diagnostic should probe conditions in the compressed target corresponding to times of peak neutron and consequently knock-on production, this quenching can result in different conditions probed experimentally by the diagnostic relative to 1-D simulations. For the purpose of studying the feasibility of the diagnostic in the presence of such mixing, we assume that the effect of the deviations from 1-D is to exclusively change the neutron-production rate and hence the knock-on spectrum. Effects on the hydrodynamic evolution of the target due to instabilities and other reasons for departures from 1-D behavior are ignored.

To assess the effect of this mixing, we compare the spectra from purely 1-D simulations with two models of neutron-rate truncation. These models should span the extremes of possible neutron-rate truncations in the experiment. In the first model, we assume that a portion of the fuel implodes with a constant velocity acquired just before deceleration begins and is unaffected by the growing instabilities at the fuel–shell interface. We then assume that the only neutron yield is from this portion of the fuel. The neutron rate from this model is shown in Fig. 9(a) as the ''free-fall'' rate and is significantly lower in magnitude relative to the 1-D simulation. Figure 9(b) shows the corresponding areal densities in the target from the simulation. As Figs. 9(a) and 9(b) indicate, the neutron rate in this model peaks earlier and thus probes earlier times in the implosion. This results in a deuteron spectrum (dotted line in Fig. 10) that is characteristic of smaller areal densities for all three layers. Our analysis of this spectrum provides values that agree reasonably with the
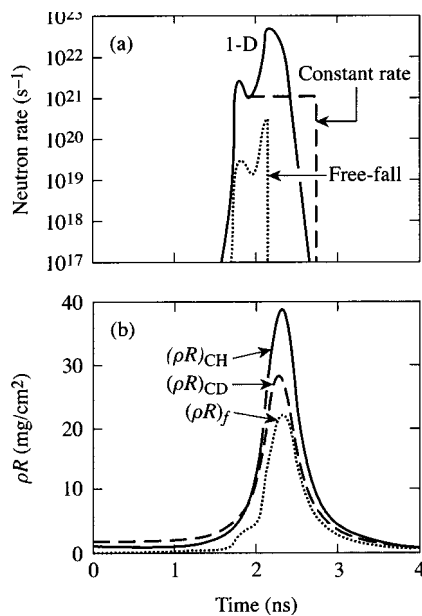
FIG. 9. (a) Neutron-rate curves for different models used for assessing the modification of the deuteron spectrum due to hydrodynamic mix: solid line—result of a 1-D simulation; dotted line—neutron rate obtained from a free-fall model (see text); and dashed line—neutron rate fixed to a constant value at a certain time. (b) ρR history of the target from 1-D simulations. The diagnostic is sensitive to areal densities near peak neutron rates and consequently to peak temperature.

results from simulation; the least-squares values are 9.8, 22.5, and 17.1 mg/cm^2, whereas the results of the simulation are 8.9, 26.7, and 15.8 mg/cm^2. We once again note that an independent measurement of $(\rho R)_{CH}$ using the knock-on proton spectrum can constrain the areal density of plastic inferred from the deuteron spectrum. The favorable comparison between the values of the areal densities inferred from the diagnostic and the true values suggests that the areal densities can still be deduced reasonably if such a modified spectrum was the result of a measurement.

In a different model, we assume that the neutron rate proceeds as given by the 1-D simulation up to a certain time, and, thereafter, it proceeds at a constant rate given by the rate at the chosen time. This is shown in Fig. 9(a) as the ''constant rate'' model. A comparison with Fig. 9(b) indicates that the diagnostic then probes the times corresponding to the
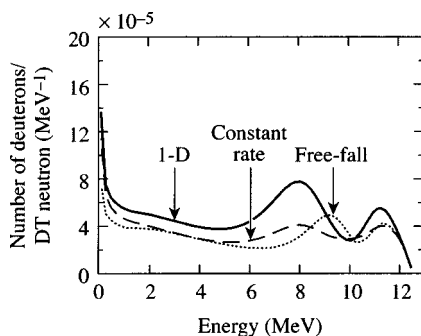

FIG. 10. Knock-on deuteron spectra using the three models of neutron-rate truncation shown in Fig. 9(a): The spectrum is sensitive to the different conditions in the compressed target probed by the deuterons.

large changes in the areal density that results in a considerably broadened emergent spectrum with less-well-defined peaks (dashed line in Fig. 10). The least-squared values (8.9, 22.9, and 18.7 mg/cm^2) are within 20% of the results of the simulation (10.7, 32.3, and 16.0 mg/cm^2), suggesting that our analysis can be used to infer the areal density of each of the layers.

The inferred ρR describe neutron-averaged conditions in the target that are very similar between the two mix scenarios described earlier. This leads to similar values of inferred areal densities. However, the mix-related information is encoded in the different spectral shapes. The spectra shown in Fig. 10 can be distinguished using the CPS since the energy resolution of the CPS for the deuterons is approximately 150 keV,[11] but mix-related information from the measured spectrum can be extracted only through additional modeling.

Experimentally, the neutron-rate history can be obtained through the neutron temporal diagnostic (NTD).[9] One method to compare the implosion with 1-D simulations could be as follows: The experimentally obtained neutron-rate curve could be used to identify the times in the implosion probed by the diagnostic—the diagnostic probes times around the peak neutron burn rate. An identification of these times would allow us to calculate the areal densities of the three layers from the simulation. A comparison of these values with those obtained from the knock-on diagnostic would shed light on whether conditions in the experiment compare favorably with the 1-D simulation up to the time probed by the diagnostic. If the areal densities inferred from the diagnostic differ considerably from those in the simulation, this procedure will allow one to identify a time when mixing effects have already significantly influenced the fusion processes. Independent of any comparison with detailed hydrodynamics simulations, the areal densities deduced from the knock-on deuteron diagnostic should be nearly model independent and would provide information about the conditions in the target corresponding to times in the implosion identified using the NTD. Further, a comparison with detailed mixing models may enable the identification of conditions in the target that would result in the observed neutron-rate curves and the inferred values of (ρR).

V. SUMMARY AND CONCLUSIONS

In this article, we have presented a new diagnostic based on knock-on deuterons, which will simultaneously diagnose the areal densities in three different regions of the compressed ICF target. These targets have three layers (DT, CH, and CD), and the areal density of each of these layers can be inferred from the deuteron diagnostic. In addition, knock-on protons from the CH layer can be used to independently deduce the areal density of the plastic.

When used in conjunction with a detector that measures the neutron-rate history of an implosion (NTD), the time in the implosion probed by this diagnostic can be identified. This will permit a more detailed comparison between the simulation and experiment.

We have also examined the modification of the knock-on deuteron spectrum caused by departures from 1-D behavior

such as mixing. Even though the spectrum can be influenced significantly by such departures from 1-D behavior, the method for analyzing the experimental spectrum should still reliably infer the areal densities in the three layers. Detailed mixing models would be required, however, to make any inferences about the mixing process in the implosions. Experiments to measure these spectra from an imploding target are currently underway, and the results will be presented elsewhere.[11]

ACKNOWLEDGMENTS

[1] G. S. Fraley, E. J. Linnebur, R. J. Mason, and R. L. Morse, Phys. Fluids **17**, 474 (1974).

[2] S. Skupsky and S. Kacenjar, J. Appl. Phys. **52**, 2608 (1981).

[3] F. J. Marshall, S. A. Letzring, C. P. Verdon, S. Skupsky, R. L. Keck, J. P. Knauer, R. L. Kremens, D. K. Bradley, T. Kessler, J. Delettrez, H. Kim, J. M. Soures, and R. L. McCrory, Phys. Rev. A **40**(5), 2547 (1989); R. L. McCrory, J. M. Soures, C. P. Verdon, F. J. Marshall, S. A. Letzring, S. Skupsky, T. J. Kessler, R. L. Kremens, J. P. Knauer, H. Kim, J. Delettrez, R. L. Keck, and D. K. Bradley, Nature (London) **335**(6187), 225 (1988).

[4] M. D. Cable and S. P. Hatchett, J. Appl. Phys. **62**, 2233 (1987).

[5] H. Nakaishi, N. Miyanaga, H. Azechi, M. Yamanaka, T. Yamanaka, M. Takagi, T. Jitsuno, and S. Nakai, Appl. Phys. Lett. **54**, 1308 (1989).

[6] D. K. Bradley, J. A. Delettrez, R. Epstein, R. P. J. Town, C. P. Verdon, B. Yaakobi, S. Regan, F. J. Marshall, T. R. Boehly, J. P. Knauer, D. D. Meyerhofer, V. A. Smalyuk, W. Seka, D. A. Haynes, Jr., M. Gunderson, G. Junkel, C. F. Hooper, Jr., P. M. Bell, T. J. Ognibene, and R. A. Lerche, Phys. Plasmas **5**, 1870 (1998).

[7] T. R. Boehly, D. L. Brown, R. S. Craxton, R. L. Keck, J. P. Knauer, J. H. Kelly, T. J. Kessler, S. A. Kumpan, S. J. Loucks, S. A. Letzring, F. J. Marshall, R. L. McCrory, S. F. B. Morse, W. Seka, J. M. Soures, and C. P. Verdon, Opt. Commun. **133**, 495 (1997).

[8] Lord Rayleigh, Proc. London Math. Soc. **XIV**, 170 (1883); G. Taylor, Proc. R. Soc. London, Ser. A **201**, 192 (1950); R. Betti, V. Goncharov, R. L. McCrory, P. Sorotokin, and C. P. Verdon, Phys. Plasmas **3**, 2122 (1996) (and references therein).

[9] R. A. Lerche, D. W. Phillion, and G. L. Tietbohl, Rev. Sci. Instrum. **66**, 933 (1995).

[10] D. G. Hicks, C. K. Li, R. D. Petrasso, F. H. Seguin, B. E. Burke, J. P. Knauer, S. Cremer, R. L. Kremens, M. D. Cable, and T. W. Phillips, Rev. Sci. Instrum. **68**, 589 (1997).

[11] C. K. Li , private communication.

[12] P. W. McKenty, C. P. Verdon, S. Skupsky, R. L. McCrory, D. K. Bradley, W. Seka, and P. A. Jaanimagi, J. Appl. Phys. **68**(10), 5036 (1990).

[13] S. Skupsky, Phys. Rev. A **16**, 727 (1977); J. D. Jackson, *Classical Electrodynamics*, 2nd ed. (Wiley, New York, 1975); C. L. Longmire, *Elementary Particle Physics* (Wiley, New York, 1963).

[14] M. C. Richardson, P. W. McKenty, F. J. Marshall, C. P. Verdon, J. M. Soures, R. L. McCrory, O. Barnouin, R. S. Craxton, J. Delettrez, R. J. Hutchinson, P. A. Jaanimagi, R. Keck, T. Kessler, H. Kim, S. A. Letzring, D. M. Roback, W. Seka, S. Skupsky, B. Yaakobi, S. M. Lane, and S. Prussin, in *Laser Interaction and Related Phenomena*, edited by H. Hora and G. H. Miley (Plenum, New York, 1986), Vol. 7, p. 421.

[15] H. Brysk, Plasma Phys. **15**, 611 (1973).

[16] W. H. Press, S. A. Teukolsky, W. T. Vetterling, and B. P. Flannery, *Numerical Recipes in FORTRAN: The Art of Scientific Computing*, 2nd ed. (Cambridge U. P., Cambridge, England, 1992).